Use of Dialkyldithiocarbamato Complexes of Bismuth(III) for the Preparation of Nano- and Microsized Bi_2S_3 Particles and the X-ray Crystal Structures of $[Bi\{S_2CN(CH_3)(C_6H_{13})\}_3]$ and $[Bi\{S_2CN(CH_3)(C_6H_{13})\}_3(C_{12}H_8N_2)]$

Olinda C. Monteiro, Helena I. S. Nogueira, and Tito Trindade*

Department of Chemistry, University of Aveiro, 3810-193 Aveiro, Portugal

Majid Motevalli

Department of Chemistry, Queen Mary & Westfield College, Mile End Road, London E1 4NS, United Kingdom

Received December 12, 2000. Revised Manuscript Received February 24, 2001

A range of bismuth(III) dithiocarbamato complexes were prepared and characterized. The X-ray crystal structures of the compounds $[Bi\{S_2CN(CH_3)(C_6H_{13})\}_3]$ (**1**) and $[Bi\{S_2CN(CH_3)(C_6H_{13})\}_3(C_{12}H_8N_2)]$ (**2**) are reported. The preparation of Bi_2S_3 particulates using a wet chemical method and involving the thermalysis of Bi(III) dialkyldithiocarbamato complexes is described. The influence of several experimental parameters on the optical and morphological properties of the Bi_2S_3 powders was investigated. Nanosized Bi_2S_3 colloids were obtained having long-term stability and showing a blue shift on the optical band edge; the presence of particles exhibiting quantum size effects is discussed. Morphological well-defined Bi_2S_3 particles were obtained in which the fiber-type morphology is prevalent.

1. Introduction

Synthetic methods and physical properties of semiconducting nanocrystals (or quantum dots) have been the subject of active research during the past decade.[1−5] In such materials, the charge carriers are confined within what is effectively a small portion of the bulk crystalline lattice. In this size regime, quantum confinement effects are observed and the band gap of the semiconductor widens as the particle size decreases to dimensions comparable to the exciton Bohr radius.[1]

Band gap tuning in nanophase semiconductors, among other properties such as the capability for surface derivatization, has been a possibility by using a plethora of chemical methods.[1−5] Most of such synthetic methods have focused on II/VI semiconductors and on III/V semiconductors.[1−11] Semiconductors having more complex structures, such as bismuth sulfide (Bi_2S_3, *bismuthinite*), which crystallizes in a lamellar structure, have received less attention.[12−14] Macrocrystalline Bi_2S_3 has been investigated as a material for photodiode arrays and photovoltaic devices.[15,16] Besides its technological interest, it has been suggested that because of its anisotropic structure, layers of lamellar semiconductors may be regarded as colloidal analogues of quantum well structures.[17,18] Therefore, quantum confinement of the charge carriers would occur, provided at least one dimension of the particles is located within the nanosize regime. Studies reporting such behavior for Bi_2S_3 have been scarce because of the lack of theoretical data and also of reliable synthetic methods that give Bi_2S_3 particulates with well-defined morphologies.

We have been interested in the preparation of nanocrystalline semiconductors using single-molecule precursors,[6,10,19] that is, molecular compounds containing

* To whom correspondence should be addressed. E-mail: ttrindade@dq.ua.pt. Fax: + 351 234 370 084.

(1) Steigerwald, M. L.; Brus, L. E. *Acc. Chem. Res*. **1990**, *23*, 183.
(2) Fendler, J. H.; Meldrum, F. C. *Adv. Mater*. **1995**, *7*, 607.
(3) Alvisatos, A. P. *J. Phys. Chem*. **1996**, *100*, 13226.
(4) Weller, H. *Adv. Mater*. **1993**, *5*, 88.
(5) Hagfeldt, A.; Grätzel, M. *Chem. Rev*. **1995**, *95*, 49.
(6) Trindade, T.; O'Brien, P.; Zhang, X. *Chem. Mater*. **1997**, *9*, 523.
(7) Trindade, T.; O'Brien, P. *Adv. Mater*. **1996**, *8*, 161.
(8) Khan-Lodhi, A.; Robison, B. H.; Towey, T.; Herramann, C.; Knoche, W.; Thesing, U. In *Structure, Dynamics and Equilibrium Properties of Colloid Systems*; Kluwer: Dordrecht, 1990; p 373.
(9) Murry, C. B.; Norris, D. J.; Bawendi, M. G. *J. Am. Chem. Soc*. **1993**, *115*, 8706.
(10) Trindade, T.; O'Brien, P.; Zhang, X.; Motevalli, M. *J. Mater. Chem*. **1997**, *7*, 1011.
(11) Guzelian, A.; Katari, J.; Kadavanich, A.; Banin, U.; Hanad, K.; Juban, E.; Alvisatos, A. P.; Wolters, R.; Arnold, C.; Heath, J. *J. Phys. Chem*. **1996**, *100*, 7212.
(12) Variano, B. F.; Hwang, D. M.; Sandroff, C. J.; Wiltzius, P.; Jing, T. W.; Ong, N. P. *J. Phys. Chem*. **1987**, *91*, 6455.
(13) Lifshitz, E.; Yassen, M.; Bykov, L.; Dag, I.; Chaim, R. *J. Phys. Chem*. **1994**, *98*, 1459.
(14) Mu, R.; Tung, Y. S.; Ueda, A.; Henderson, D. O. *J. Phys. Chem*. **1996**, *100*, 19927.
(15) Pawar, S. H.; Bhosale, P. N.; Uplane, M. D.; Tamhankar, S. *Thin Solid Films* **1983**, *110*, 165.
(16) Killedar, V. V.; Lokhande, C. D.; Bhosale, C. H. *Thin Solid Films* **1996**, *289*, 14.
(17) Sandroff, C. J.; Hwang, D. M.; Chung, W. M. *Phys. Rev. B* **1986**, *33*, 5953.
(18) Sandroff, C. J.; Kelty, S. P.; Hwang, D. M. *J. Chem. Phys.* **1986**, *85*, 5337.
(19) Trindade, T.; Monteiro, O. C.; O'Brien, P.; Motevalli, M. *Polyhedron* **1999**, *18*, 1171.

10.1021/cm000973y CCC: $20.00
Published on Web 05/11/2001

both elements of the semiconductor within a single molecule, for example, metal dithiocarbamato complexes. The use of tris(benzylthiolato)bismuth to produce pure polycrystalline Bi_2S_3 is reported in the literature.[20] Recently, we showed that the compound bismuth(III) methyl-*n*-hexyl-dithiocarbamate ([Bi{$S_2CN(CH_3)(C_6H_{13})$}$_3$]) is a useful single-molecule precursor to produce fiber-type Bi_2S_3 particles, either in organic solution[21] or by a CVD method.[22] Here, we report a more detailed study using other single-molecule precursors to prepare nano- and microcrystalline Bi_2S_3 powders by thermalysis in high boiling point solvents. The influence of several synthetic parameters on the final morphological and optical properties of the powders is reported.

Moreover, our interest in the production of Bi_2S_3 materials using such compounds led us to investigate some structural features inherent to bismuth(III) dithiocarbamato complexes, in particular, the asymmetric alkyl derivatives. Bismuth(III) dithiocarbamato complexes have been known for a long time and crystal structures have been reported for [$Bi(S_2CNEt_2)_3$][23] and a number of [$Bi(S_2CNEt_2)_3$] halogen substituted complexes.[24−28] Here are reported for the first time X-ray crystal structures of asymmetric bismuth(III) *N*,*N*-dialkyl dithiocarbamato complexes, namely, for the compounds [Bi{$S_2CN(CH_3)(C_6H_{13})$}$_3$] (**1**) and [Bi{$S_2CN(CH_3)(C_6H_{13})$}$_3$($C_{12}H_8N_2$)] (**2**).

2. Experimental Section

All chemicals were supplied by Aldrich except Bi_2O_3 and dry methanol (Merck), and toluene and 2-ethoxyethanol (Riedel & Haan). All chemicals were used as received.

2.1. Synthesis of Bismuth(III) Dialkyldithiocarbamato Complexes. The complexes [$Bi(S_2CNMe^nHex)_3$], [$Bi(S_2CNMe^nBu)_3$], [$Bi(S_2CNEt_2)_3$], and [$Bi(S_2CN^nBu_2)_3$], in which Me = methyl, Et = ethyl, ^{n}Bu = *n*-butyl, and ^{n}Hex = *n*-hexyl, were prepared by adaptation of the literature method.[29] The synthetic method consists of the insertion of CS_2 into the secondary amine in the presence of Bi_2O_3. In a typical synthesis, [$Bi(S_2CNMe^nHex)_3$] was obtained by adding dropwise *N*-methylhexylamine, 98% (40 mmol), and then CS_2 (40 mmol) to a methanol suspension of Bi_2O_3 (6 mmol; 20 mL). The mixture continued to react with stirring, at room temperature, over 24 h. The yellow solid formed was collected by filtration and the product recrystallized from a hot chloroform:methanol mixture (3:1). All bismuth(III) complexes were prepared similarly using the respective secondary amine. The compound [$Bi(S_2CNMe^nHex)_3(C_{12}H_8N_2)$] was obtained by stirring an acetone solution (50 mL) containing [$Bi(S_2CNMe^nHex)_3$] (0.40 g) and *o*-phenanthroline: $C_{12}H_8N_2$ (0.2 g) over 2 h; the pale yellow solid formed was recrystallized from hot acetone. All compounds were characterized by NMR and IR spectroscopies and microanalysis.

[$Bi(S_2CNMe^nHex)_3$]. ^{1}H NMR: δ 0.89 [3H, t, $(CH_2)_5CH_3$]; δ 1.31 [6H, t, $(CH_2)_2(CH_2)_3CH_3$]; δ 1.74 [2H, m, $CH_2CH_2(CH_2)_3CH_3$]; δ 3.36 [3H, s, CH_3]; δ 3.78 [2H, t, $CH_2(CH_2)_4CH_3$]. ^{13}C NMR: δ 13.96 [$(CH_2)_5CH_3$]; δ 22.51[$(CH_2)_4CH_2CH_3$]; δ 26.43 [$(CH_2)_3CH_2CH_2CH_3$]; δ 26.79 [$(CH_2)_2CH_2(CH_2)_2CH_3$]; δ 31.40 [$CH_2CH_2(CH_2)_3CH_3$]; δ 41.80 [CH_3]; δ 56.67 [$CH_2(CH_2)_4CH_3$]; δ 201.41 [S_2CN]. Elemental analysis (%). Found: C, 35.66; H, 5.51; N, 5.20; S, 24.45. Calcd: C, 36.97; H, 6.16; N, 5.39; S, 24.65. IR major bands (ν/cm^{-1}): 1491 [ν(C−N)], 957 [ν(C−S)]. Yield 70%. mp 105 °C.

[$Bi(S_2CNMe^nBu)_3$]. ^{1}H NMR: δ 0.94 [3H, t, $(CH_2)_3CH_3$]; δ 1.35 [2H, m, $(CH_2)_2CH_2CH_3$]; δ 1.73 [2H, m, $CH_2CH_2CH_2CH_3$]; δ 3.36 [3H, s, CH_3]; δ 3.79 [2H, t, $CH_2(CH_2)_2CH_3$]. ^{13}C NMR: δ 13.74 [$(CH_2)_3CH_3$]; δ 20.02 [$(CH_2)_2CH_2CH_3$]; δ 28.87 [$CH_2CH_2CH_2CH_3$]; δ 56.44 [$CH_2(CH_2)_2CH_3$]; δ 201.42 [S_2CN]. Elemental analysis (%). Found: C, 30.21; H, 4.76; N, 5.91; S, 29.50. Calcd: C, 31.08; H, 5.18; N, 6.04; S, 27.63. IR major bands (ν/cm^{-1}): 1488 [ν(C−N)], 953 [ν(C−S)]. Yield 91%. mp 143 °C.

[$Bi(S_2CNEt_2)_3$]. ^{1}H NMR: δ 1.33 [6H, t, CH_2CH_3]; δ 3.83 [4H, q, CH_2CH_3]. ^{13}C NMR: δ 12.21 [CH_2CH_3]; δ 48.30 [CH_2CH_3]; δ 200.46 [S_2CN]. Elemental analysis (%). Found: C, 26.82; H, 4.13; N, 6.29; S, 31.65. Calcd: C, 27.56; H, 4.59; N, 6.43; S, 29.40. IR major bands (ν/cm^{-1}): 1490 [ν(C−N)], 983 [ν(C−S)]. Yield 45%. mp 201 °C.

[$Bi(S_2CN^nBu_2)_3$]. ^{1}H NMR: δ 0.94 [3H, t, $(CH_2)_3CH_3$]; δ 1.34 [2H, m, $(CH_2)_2CH_2CH_3$]; δ 1.75 [2H, m, $CH_2CH_2CH_2CH_3$]; δ 3.73 [2H, t, $CH_2(CH_2)_2CH_3$]. ^{13}C NMR, δ 13.71 [$(CH_2)_3CH_3$]; 20.11[$(CH_2)_2CH_2CH_3$]; δ 28.92 [$CH_2CH_2CH_2CH_3$]; δ 53.94 [$CH_2(CH_2)_2CH_3$]; δ 200.90 [S_2CN]. Elemental analysis (%). Found: C, 38.29; H, 5.91; N, 4.95; S, 24.44. Calcd: C, 39.46; H, 6.58; N, 5.12; S, 23.39. IR major bands (ν/cm^{-1}): 1483 [ν(C−N)], 956 [ν(C−S)]. Yield 56%. mp 99 °C.

[$Bi(S_2CNMe^nHex)_3(C_{12}H_8N_2)$]. ^{1}H NMR: δ 0.88 [3H, t, $(CH_2)_5CH_3$]; δ 1.30 [6H, t, $(CH_2)_2(CH_2)_3CH_3$]; δ 1.73 [2H, m, $CH_2CH_2(CH_2)_3CH_3$]; δ 3.35 [3H, s, CH_3]; δ 3.78 [2H, t, $CH_2(CH_2)_4CH_3$]. The following peaks are due to the *o*-phenanthroline ligand: δ 7.62 [H, q]; δ 7.77 [H, s]; δ 8.23 [H, t]; δ 9.19 [H, t]. ^{13}C NMR: δ 13.98 [$(CH_2)_5CH_3$]; δ 22.52 [$(CH_2)_4CH_2CH_3$]; δ 26.42 [$(CH_2)_3CH_2CH_2CH_3$]; δ 26.83 [$(CH_2)_2CH_2(CH_2)_2CH_3$]; δ 31.42 [$CH_2CH_2(CH_2)_3CH_3$]; δ 41.74 [CH_3]; δ 56.59 [$CH_2(CH_2)_4CH_3$]; δ 201.48 [S_2CN]. The following peaks are due to the *o*-phenathroline ligand: δ 123.04; δ 126.49; δ 128.60; δ 135.97; δ 146.17; δ 150.41. IR bands (ν/cm^{-1}) (major bands): 1486 [ν(C−N)], 974 [ν(C−S)]. Yield 56%. mp 144 °C.

2.2. Preparation of Bi_2S_3 Particulates. Bi_2S_3 particulates were prepared by solution thermalysis of the bismuth(III) dithiocarbamate complexes. The decomposition of such compounds was performed in the solvents *p*-xylene, 4-ethylpyridine, 2-ethoxyethanol, ethyleneglycol (1,2-dihydroxyethane), and tri-*n*-octylphosphine oxide, which were flushed with N_2 prior to use. All the reactions were performed under a N_2 stream, using a round flask heated by an oil bath at the required temperature and equipped with a Liebig condenser. The experimental apparatus was placed inside a fume cupboard equipped with local exhaust ventilation. For each solvent the thermalysis was performed as follows:

Tri-n-octylphosphine oxide (TOPO). [$Bi(S_2CNRR')_3$] (0.2 mmol) was dissolved in 10 mL of tri-*n*-octylphosphine (TOP). This solution was carefully injected into 25 g of TOPO, while stirring, at 150 °C over 2 h. The mixture was then cooled to 60 °C and an excess of methanol was added. The powder obtained was isolated by centrifugation and washed with methanol.

2-Ethoxyethanol. A solution of the precursor (0.20 mmol) in 2-ethoxyethanol (50 mL) was refluxed (132 °C) over 2 h. The solution was then left to cool to room temperature The solid formed was isolated by centrifugation and washed with *n*-hexane. The dark powder obtained was dispersed in organic solvents such as dichlorometane, pyridine, and acetone.

Ethyleneglycol, 4-Ethylpyridine, and p-Xylene. The thermalysis of the bismuth complexes using these solvents was performed at the solvent reflux temperature, using a procedure similar to the one used with 2-ethoxyethanol. The powders obtained in the presence of ethyleneglycol were washed with

(20) Boudjouk, P.; Remington, M. P., Jr.; Grier, D. G.; Jarabek, B. R.; McCarthy, G. J. *Inorg. Chem.* **1998**, *37*, 3538.
(21) Monteiro, O. C.; Trindade, T. *J. Mater. Sci. Lett.* **2000**, *19*, 859.
(22) Monteiro, O. C.; Trindade, T.; Park, J.-H.; O'Brien, P. *Chem. Vap. Dep.* **2000**, *6*, 230.
(23) Raston, C. L.; White, A. H. *J. Chem. Soc., Dalton* **1976**, 791.
(24) Raston, C. L.; Rowbottom, G. L.; White, A. H. *J. Chem. Soc., Dalton* **1981**, 1352.
(25) Raston, C. L.; Rowbottom, G. L.; White, A. H. *J. Chem. Soc., Dalton* **1981**, 1366.
(26) Raston, C. L.; Rowbottom, G. L.; White, A. H. *J. Chem. Soc., Dalton* **1981**, 1369.
(27) Raston, C. L.; Rowbottom, G. L.; White, A. H. *J. Chem. Soc., Dalton* **1981**, 1379.
(28) Raston, C. L.; Rowbottom, G. L.; White, A. H. *J. Chem. Soc., Dalton* **1981**, 1383.
(29) Nomura, R.; Kanaya, K.; Matsuda, H. *Bull. Chem. Soc. Jpn.* **1989**, *62*, 939.

Table 1. Crystal Data and Structure Refinement of [Bi($S_2CNMe^nHex)_3$] and [Bi($S_2CNMe^nHex)_3(C_{12}H_8N_2$)]

empirical formula	$C_{24}H_{48}BiN_3S_6$	$C_{36}H_{56}BiN_5S_6$
formula weight	779.99	960.20
temperature	293(2) K	180(2) K
wavelength	0.71073 Å	0.71073 Å
crystal system	monoclinic	triclinic
space group	*P*21/*c*	*P*1
unit cell dimensions	$a = 19.833(3)$ Å, $\alpha = 90°$	$a = 10.401(8)$ Å, $\alpha = 105.36(5)°$
	$b = 17.423(3)$ Å, $\beta = 104.57(2)°$	$b = 14.598(9)$ Å, $\beta = 80.64(6)°$
	$c = 10.145(2)$ Å, $\gamma = 90°$	$c = 15.341(9)$ Å, $\gamma = 108.19(5)°$
volume	3392.9(10) Å^3	2126(2) Å^3
Z	4	2
density (calculated)	1.527 Mg/m^3	1.500 Mg/m^3
absorption coefficient	5.583 mm^{-1}	4.473 mm^{-1}
F(000)	1568	972
crystal size	0.2 × 0.2 × 0.1 mm^3	0.4 × 0.3 × 0.2 mm^3
θ range for data collection	1.58°−24.98°	1.51°−25.10°
index ranges	$0 \le h \le 23, 0 \le k \le 20$	$-1 \le h \le 12, -17 \le k \le 16$
	$-12 \le l \le 11$	$-17 \le l \le 18$
reflections collected	6119	8198
independent reflections	5940 [*R*(int) = 0.0527]	7500 [*R*(int) = 0.0372]
completeness to $\theta = 24.98°$	99.8%	98.8%
refinement method	full-matrix least-squares on F^2	full-matrix least-squares on F^2
data/ restrains/parameters	5940/90/313	7500/9/439
goodness-of-fit on F^2	1.007	1.001
final *R* indices [$I > 2\sigma(I)$]	R1 = 0.0591, wR2 = 0.1720	R1 = 0.0395, wR2 = 0.1015
R indices (all data)	R1 = 0.1414, wR2 = 0.2364	R1 = 0.0518, wR2 = 0.1053
largest diff peak and hole	2.668 and −2.754 e·Å^{-3}	1.306 and −1.259 e·Å^{-3}

methanol and then dispersed in solvents such as dichloromethane or pyridine. When 4-ethylpyridine was used as the solvent, the powder obtained was washed with *n*-hexane and dispersed in dichloromethane. The decomposition of the bismuth complexes in *p*-xylene resulted in the formation of a powder that did not disperse in organic solvents.

2.3. Instruments and Characterization. *Crystallography*. The intensity data were collected on an Enraf Nonius CAD-4 diffractometer using Mo Kα radiation ($\lambda = 0.71069$ Å) with an $\omega-2\theta$ scan at 180 K. The unit cell parameters were determined by least-squares refinement on diffractometer angles $9.38° \le \theta \le 12.15°$ (**1**) and $8.411° \le \theta \le 12.72°$ (**2**) for 25 automatically centered reflections in each case.[30] Crystal data are summarized in Table 1. All data were corrected for absorption by semiempirical methods (ψ scan)[31] and for Lorentz-polarization effects by XCAD4.[32] The structure was solved by the Patterson method using SHELXS-97[33] and refined anisotropically (non-hydrogen atoms) by full-matrix least-squares on F^2 using the SHELXL-97 program.[33] The H atoms were calculated geometrically and refined with a riding model. The program ORTEP-3[34] was used for drawing the molecules. WINGX[35] was used to prepare material for publication.

Spectroscopic Methods. The UV/visible absorption spectra were recorded on a Jasco V-560 UV/VIS spectrophotometer, using quartz cuvettes and the respective solvent as reference. The NMR spectra were recorded on a Bruker AMX 300 spectrometer using $CDCl_3$ + TMS solutions. The infrared spectra were recorded on a Matson 700 FTIR Spectrometer using dry KBr disks.

Powder Diffraction and Microscopy Techniques. X-ray powder diffraction (XRD) was performed on powders deposited on silicon substrates, using a Philips X'Pert instrument operating with Cu Kα radiation ($\lambda = 1.54178$ Å) at 40 kV/50 mA.

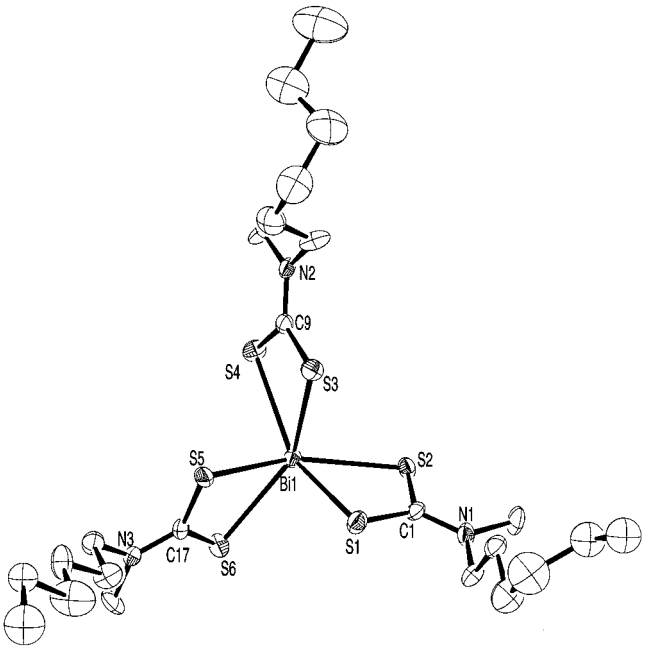

Figure 1. Molecular structure of [Bi($S_2CNMe^nHex)_3$].

Transmission electron microscopy (TEM) was carried out on a Hitachi H-9000 microscope operating at 300 kV. An aliquot containing the nanodispersed sample was placed on a copper grid coated with an amorphous carbon film and then the solvent was evaporated.

Scanning electron microscopy (SEM) images and energy-dispersive X-ray (EDAX) measurements results were obtained using a FEG-SEM Hitachi S4100 microscope operating at 25 kV. The samples were prepared by deposition of an aliquot of the sample on aluminum pieces.

3. Results and Discussion

3.1. Crystal Structures. The molecular structure of [Bi($S_2CNMe^nHex)_3$] (**1**) is shown in Figure 1. The complex comprises a bismuth atom coordinated by three bidentate asymmetric methyl-*n*-hexyl dithiocarbamato ligands. Selected bond lengths and angles for this

(30) Enraf-Nonius *CAD-4/PC Software, Version 1.5c*; Enraf-Nonius: Delft, The Netherlands, 1992.
(31) North, A. C. T.; Phillips, D. C.; Mathews, F. S. *Acta Crystalloger., Sect. A* **1968**, *42*, 351−359.
(32) Harms, K. *XCAD4. Program for data reduction*; Philipps-Universität, Marburg, Germany, 1996.
(33) Sheldrick, G. M. *SHELX-97 Program for solution and refinement of crystal structures*; University Gottingen: Germany, 1997.
(34) Farrugia, L. J. *ORTEP-3 for Windows. J. Appl. Cryst.* **1997**, *30*, 565.
(35) Farrugia, L. J., WinGX−*A Windows Program for Crystal Structure Analysis*; University of Glasgow: Glasgow, 1998.

Table 2. Selected Bond Lengths (Å) and Angles (deg) for [Bi(S_2CNMe^nHex)$_3$] and [Bi(S_2CNMe^nHex)$_3$($C_{12}H_8N_2$)]

		1	
Bi(1)−S(3)	2.741(2)	Bi(1)−S(2)	2.868(2)
Bi(1)−S(1)	2.694(3)	Bi(1)−S(6)	2.882(3)
Bi(1)−S(5)	2.679(2)	Bi(1)−S(4)	2.889(2)
S(5)−Bi(1)−S(1)	87.27(8)	S(1)−Bi(1)−S(6)	95.88(8)
S(5)−Bi(1)−S(3)	81.94(7)	S(3)−Bi(1)−S(6)	146.17(7)
S(1)−Bi(1)−S(3)	86.01(7)	S(2)−Bi(1)−S(6)	117.82(7)
S(5)−Bi(1)−S(2)	152.12(7)	S(5)−Bi(1)−S(4)	94.69(7)
S(1)−Bi(1)−S(2)	64.92(7)	S(1)−Bi(1)−S(4)	148.75(7)
S(3)−Bi(1)−S(2)	93.63(7)	S(3)−Bi(1)−S(4)	63.52(7)
S(5)−Bi(1)−S(6)	64.48(7)	S(2)−Bi(1)−S(4)	107.99(7)
		S(6)−Bi(1)−S(4)	113.12(7)
		2	
Bi(1)−S(3)	2.700(3)	Bi(1)−N(5)	2.836(5)
Bi(1)−N(4)	2.776(5)	Bi(1)−S(2)	2.848(2)
Bi(1)−S(1)	2.779(2)	Bi(1)−S(6)	2.900(2)
Bi(1)−S(5)	2.794(2)	Bi(1)−S(4)	2.966(3)
S(3)−Bi(1)−N(4)	160.07(11)	N(5)−Bi(1)−S(2)	77.06(11)
S(3)−Bi(1)−S(1)	82.29(7)	S(3)−Bi(1)−S(6)	100.45(7)
N(4)−Bi(1)−S(1)	83.41(12)	N(4)−Bi(1)−S(6)	81.66(12)
S(3)−Bi(1)−S(5)	84.12(8)	S(1)−Bi(1)−S(6)	139.28(6)
N(4)−Bi(1)−S(5)	79.24(12)	S(5)−Bi(1)−S(6)	62.84(6)
S(1)−Bi(1)−S(5)	77.25(7)	N(5)−Bi(1)−S(6)	81.78(11)
S(3)−Bi(1)−N(5)	141.50(11)	S(2)−Bi(1)−S(6)	155.52(5)
N(4)−Bi(1)−N(5)	58.38(15)	S(3)−Bi(1)−S(4)	62.90(7)
S(1)−Bi(1)−N(5)	120.79(11)	N(4)−Bi(1)−S(4)	136.77(11)
S(5)−Bi(1)−N(5)	128.39(11)	S(1)−Bi(1)−S(4)	130.52(6)
S(3)−Bi(1)−S(2)	88.80(8)	S(5)−Bi(1)−S(4)	128.01(7)
N(4)−Bi(1)−S(2)	97.32(12)	N(5)−Bi(1)−S(4)	79.36(12)
S(1)−Bi(1)−S(2)	64.06(7)	S(2)−Bi(1)−S(4)	80.31(8)
S(5)−Bi(1)−S(2)	141.26(6)	S(6)−Bi(1)−S(4)	83.85(8)

Table 3. Comparative Bond Distances for Group 15 Metal Dithiocarbamato Complexes: M−S_A and M−S_B Refer to the Shorter and Longer Distances, Respectively

compound	M−S_A/Å	M−S_B/Å	Δ ((M−S_B) − (M−S_A))/Å
[As(S_2CNEt_2)$_3$][a]	2.350	2.904	0.554
	2.344	2.819	0.475
	2.354	2.812	0.458
[Sb(S_2CNEt_2)$_3$][b]	2.631	2.886	0.255
	2.487	2.965	0.478
	2.626	2.895	0.269
[Bi(S_2CNEt_2)$_3$][b]	2.595	2.956	0.361
	2.775	2.964	0.189
	2.730	2.908	0.178
[Bi($S_2CNMeHex$)$_3$]	2.679	2.885	0.206
	2.694	2.868	0.174
	2.741	2.889	0.148
[Bi($S_2CNMeHex$)$_3$($C_{12}H_8N_2$)]	2.700	2.966	0.266
	2.794	2.900	0.106
	2.779	2.848	0.069

[a] Data from ref 36. [b] Data from ref 23.

compound are summarized in Table 2. The Bi—S bonds for each dithiocarbamato ligand are asymmetric but such asymmetry is not so accentuated as in the reported structures for diethyldithiocarbamato complexes of Bi, As, and Sb.[23,36,37] Comparative bond distances for metal dithiocarbamato complexes are listed in Table 3. Nevertheless, as described for the complex [As(S_2CNEt_2)$_3$],[37] it is possible to recognize two triangular faces on the coordination polyhedron defined by the three Bi—S short bonds (2.679−2.741 Å) and by the remaining three Bi—S longer bonds (2.868−2.889 Å), both perpendicular to a pseudorotation 3-fold axis. Such an arrangement results in a distorted coordination environment around the metal center, which is best described as a distorted triangular antiprism. The distortion on the coordination polyhedron by elongation of the Bi—S bonds of one of the triangular faces of the triangular antiprism may result from the presence of a stereochemically active electron lone pair along the pseudo-3-fold axis and directed to the larger triangular face. The presence of the stereochemically active electron lone pair is also suggested by the bigger angles S—Bi—S involving the three Bi—S longer bonds (107.99°−117.82°), when compared to the S—Bi—S angles involving the three Bi—S short bonds (81.94°−87.27°). It must be emphasized that, in such a case, the electronic repulsion effects of the electron lone pair on the coordination geometry of the metal center are less pronounced than those described for [Bi(S_2CNEt_2)$_3$][23] and for [As(S_2CNEt_2)$_3$].[37] A comparison of the molecular structures of [Bi(S_2CNEt)$_3$][23] and [Bi($S_2CNMeHex$)$_3$] is elucidative with respect to the observation of different coordination geometries for the bismuth by introducing subtle differences in the ligands as it is the case of replacing the ethyl groups by an asymmetric set formed by short-chain (methyl) and long-chain (*n*-hexyl) alkyl groups. In the compound [Bi(S_2CNEt_2)$_3$],[23] the bismuth coordination sphere is completed by the close proximity of a S atom from a neighboring molecule at a distance (3.210 Å) less than the sum of the van der Waals radii.[38] The bismuth stereochemistry has been described for such compounds as a distorted dodecahedron by taking in account the presence of an active electron lone pair.[23] It is apparent from Figure 1 that a distinct stereochemistry is present for bismuth in compound **1**. Unlike the complex [Bi(S_2CNEt_2)$_3$], compound **1** consists of discrete units in which intermolecular contacts, comprising the metal center, within adjacent molecules are not present. This can be associated with the lengthening of a substituent alkyl group from a two-carbon chain to a six-carbon chain, resulting in a distinct molecular packing to accommodate the longer hexyl chain. The nonexistence of intermolecular contacts involving the metal center favors in this case a less distorted coordination geometry.

A few bismuth *N*,*N*-diethyldithiocarbamato complexes containing nitrogen donors in the coordination sphere have been reported by Raston et al.[27,28] Because of the Lewis acidic character and large size of bismuth, the expansion of the coordination number of dithiocarbamato bismuth complexes in the presence of Lewis bases is favored. However, there are no reports on the structural characterization of such types of complexes in which the alkyl chains of the dithiocarbamato ligands are asymmetric. Figure 2 shows the molecular structure of the compound [Bi($S_2CNMeHex$)$_3$($C_{12}H_8N_2$)] (**2**). Bismuth is coordinated by three asymmetric bidentate dithiocarbamato ligands and the coordination sphere is expanded in this case by chelation of an *o*-phenantroline molecule leading to a complex with coordination number 8. The Bi—S distances are within the typical values found for this type of compound. The Bi—N interactions are inferior to the sum of the van der Waals radii (<4 Å) and within the range found for Bi—N distances in

(36) Raston, C. L.; White, A. H. *J. Chem. Soc., Dalton* **1975**, 2425.
(37) Colapietro, M.; Domenicano, A.; Scaramuzza, L.; Vaciago, A. *Chem. Commun.* **1968**, 302.
(38) Silvestru, C.; Breunig, H. J.; Althaus, H. *Chem. Rev.* **1999**, *99*, 3277.

Table 4. Relevant Experimental Data for the 2-h Thermalysis of [Bi(S_2CNMe^nHex)$_3$] in High Boiling Point Solvents

solvent	temp[a]/°C	solid phase[b]	observations
2-ethoxyethanol	132	Bi_2S_3	brown powder which disperses easily in hydrocarbons such as CH_2Cl_2 (leading to long-term stable dispersions)
ethylene glycol	197	Bi_2S_3	brown powder which disperses easily in hydrocarbons such as CH_2Cl_2 (leading to long-term stable dispersions)
4-ethylpyridine	168	Bi_2S_3	brown powder which disperses in hydrocarbons
p-xylene	140	Bi_2S_3	brown powder which does not disperse in organic solvents
TOPO/TOP	150	Bi_2S_3 and Bi	gray powder which disperses in hydrocarbons (leading to short-term stable dispersions)

[a] Reflux except for TOPO/TOP. [b] As determined by XRD data.

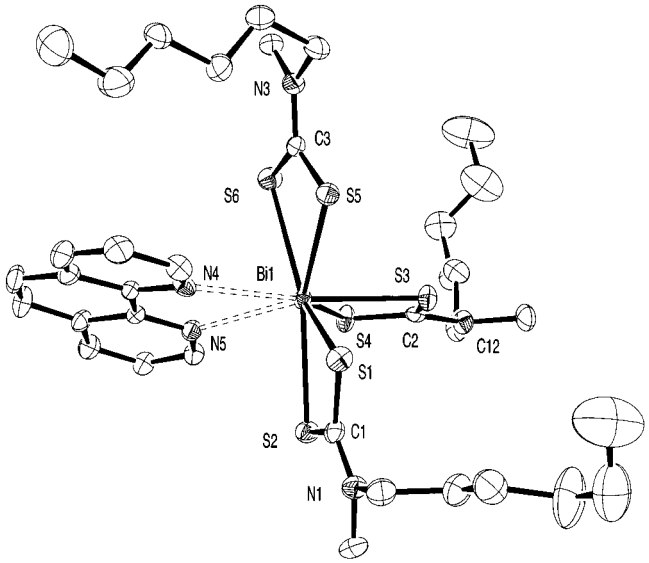

Figure 2. Molecular structure of [Bi(S_2CNMe^nHex)$_3$($C_{12}H_8N_2$)].

similar compounds.[27,28] In complex **2**, the Bi—N interactions can be considered as secondary bonds because they are longer than typical Bi—N covalent bond distances, but shorter than the sum of the van der Waals radii.[38] The Bi—S distances are in the range 2.700−2.966 Å and are close to the sum of the covalent radii of the elements (2.54 Å); therefore, the Bi—S interactions are considered primary bonds. This is consistent with the trans influence observed for a number of bismuth complexes showing secondary and primary Bi—E bonds, in which E is a nonmetal atom.[38] In fact, for compound **2**, in the set of bonds defined by the Bi, N(4), N(5), S(3), and S(4) atoms (Figure 2), the shortest secondary bond, that is, the Bi—N4 bond, is opposite the longer primary bond, that is, the Bi—S4 bond.

When compared to compound **1**, sterical hindrance due to the presence of an additional *o*-phenanthroline molecule in complex **2** forces the donor atoms to define nearly two planes containing the bismuth atom, which are almost orthogonal in relation to each other. The presence of the *o*-phenantroline molecule in a relative trans position to a dithiocarbamato ligand induces an increase in the asymmetry of the bismuth dithiocarbamato bond distances. In fact, the higher difference in the Bi—S distances is observed for the dithiocarbamato ligand trans to the phenantroline molecule in relation to the plane defined by the remaining S donor ligands. Also, in compound **2**, the coordination number of bismuth has increased to 8 in relation to the parent compound **1** and the stereochemistry is best described as a distorted dodecahedron defined by the S and N donor atoms. The distortion on the coordination geometry could also be due to the presence of an electron lone-pair stereochemically active on bismuth. The influence of the electron lone pair on the coordination geometry of bismuth is not so evident as that in the previous compound, **1**, which can be related to the expansion of the coordination number by introducing a bidentate ligand with a higher bite angle such as *o*-phenanthroline.[38] In this case, the distortion from a regular geometry is possibly due mainly to stereochemical restrictions imposed by both types of bidentate ligands with distinct bite angles.

3.2. Preparation of Bi_2S_3 Nanocrystals. The molecular precursors **1** and **2** and the complexes [Bi(S_2CNMe^nBu)$_3$], [Bi(S_2CNEt_2)$_3$], and [Bi($S_2CN^nBu_2$)$_3$] thermally decompose into pure Bi_2S_3 under a N_2 stream. This led us to investigate in detail the use of such compounds as single-molecule precursors to prepare Bi_2S_3 particulates. In a preliminary report we have described the preparation of Bi_2S_3 nanofibers in 2-ethoxyethanol using [Bi(S_2CNMe^nHex)$_3$] as a single-molecule precursor.[21] Here, a more detailed study of the solution phase thermalysis of bismuth(III) dithiocarbamato complexes is reported. Moreover, the preliminary results[21] suggested that the solvent used had a strong influence on the final properties of the Bi_2S_3 powders. In this work, the solution thermalysis of bismuth complexes was investigated using other solvents with higher boiling points and also thermally more stable than 2-ethoxyethanol.[39]

The results obtained from the solution thermal treatment of the complex [Bi(S_2CNMe^nHex)$_3$] in several solvents are summarized in Table 4. The treatment of [Bi(S_2CNMe^nHex)$_3$] in *p*-xylene led to Bi_2S_3 powders that were not dispersible in any of the organic solvents tested. This result suggested that the particles in this case were not nanosized, a result confirmed later by SEM. A possible explanation for this fact is that the Bi_2S_3 primary particles formed during the thermalysis of the precursor do not have a capped surface because *p*-xylene is not a coordinating solvent. Absence of protective agents at the surface of the Bi_2S_3 nanoparticles formed facilitates the growth into larger particles at the high temperature used.

The thermalysis of [Bi(S_2CNMe^nHex)$_3$] and [Bi(S_2CNMe^nHex)$_3$($C_{12}H_8N_2$)] in TOPO led to a mixture of Bi_2S_3 and elemental bismuth. The latter was detected in the powder as a secondary phase from XRD analysis. The other solvents tried (2-ethoxyethanol, 4-ethylpyridine, and ethyleneglycol) led to pure Bi_2S_3, which disperses in hydrocarbons. The amount of nanomaterial

(39) Vincoli, J. W. *Risk Management for Hazardous Chemicals*; CRC Press Lewis Publishers: Boca Raton, FL, 1997; Vol. 2, p 1309.

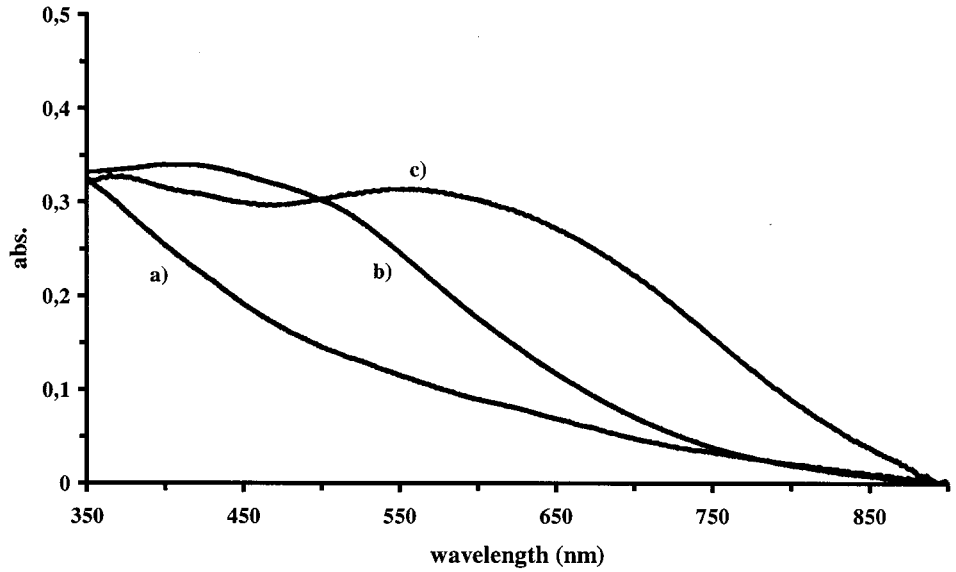

Figure 3. Optical absorption spectra of Bi_2S_3 nanodispersed in CH_2Cl_2, prepared at 132 °C in (a) 4-ethylpyridine, (b) 2-ethoxyethanol, and (c) ethyleneglycol.

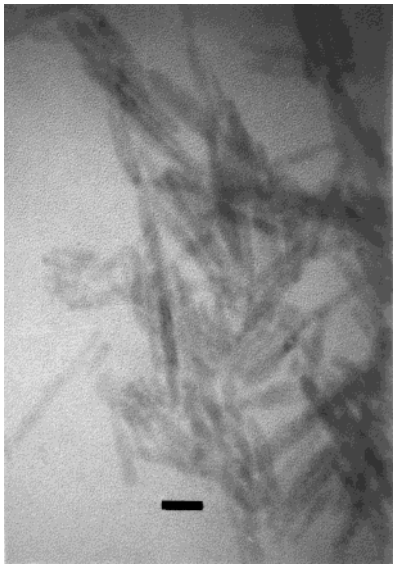

Figure 4. TEM image of Bi_2S_3 nanofibers prepared from [Bi($S_2CNMe^nHex)_3$] in 2-ethoxyethanol at 132 °C over 2 h (bar = 15 nm).

prepared in 2-ethoxyethanol was higher than those with other solvents. At room temperature, the molecular precursor [Bi($S_2CNMe^nHex)_3$] also decomposes in a 2-ethoxyethanol solution. However, the powders prepared in such conditions showed a low crystallinity degree and were obtained by stirring the solution over several days.

The optical spectra of the nanoparticulates prepared using 4-ethylpyridine, ethyleneglycol, and 2-ethoxyethanol (at 132 °C for all solvents) are shown in Figure 3. The subtle differences observed on the band profiles of the optical spectra (Figure 3) can be associated with different particle size distributions for the Bi_2S_3 particles, depending on the solvent used in their preparation. The optical band edge of Bi_2S_3 for all the samples is considerably shifted to high energy (ca. 0.6 eV) from the typical direct band gap of 1.3 eV (952 nm). As will be discussed later, this shift may be explained by the presence of Bi_2S_3 nanocrystals in which at least one linear dimension of the crystallites is nanosized.[18]

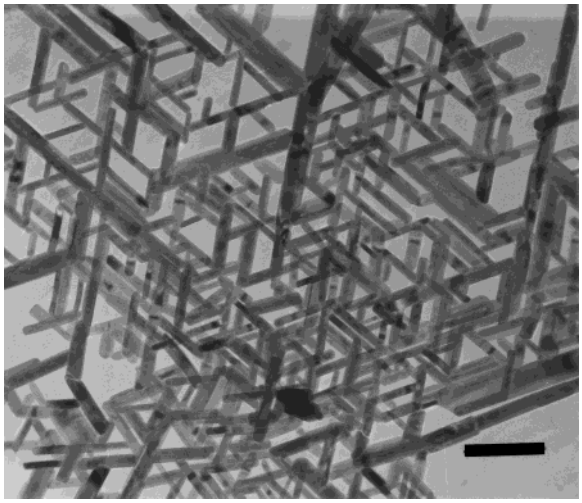

Figure 5. TEM image of Bi_2S_3 nanofibers prepared from [Bi($S_2CNMe^nHex)_3(C_{12}H_8N_2)$] in ethyleneglycol at 197 °C over 2 h (bar = 140 nm).

No meaningful distinct features were observed in the optical spectra of Bi_2S_3 prepared using distinct bismuth(III) dithiocarbamato complexes. This result suggests that the nature of the alkyl chain of the precursors reported here does not have a strong influence on the optical properties of the Bi_2S_3 that results from the thermalysis. A red shift on the optical absorption onset was clearly observed with the increase of the temperature of thermalysis, in agreement with an increase in the mean particle size, and suggesting a growth process driven by the reduction of the total surface energy of the particulates (Ostwald ripening).

3.3. Structural and Morphological Characterization of Bi_2S_3 Powders. X-ray powder diffraction performed on the powders obtained in this work showed that *bismuthinite* was the crystalline phase present in all the samples, except for those prepared in TOPO in which elemental bismuth was also detected. The IR spectra of the powders did not show organic vestiges either from the solvent or from the molecular precursor. EDAX measurements performed on the powders showed peaks for Bi and S.

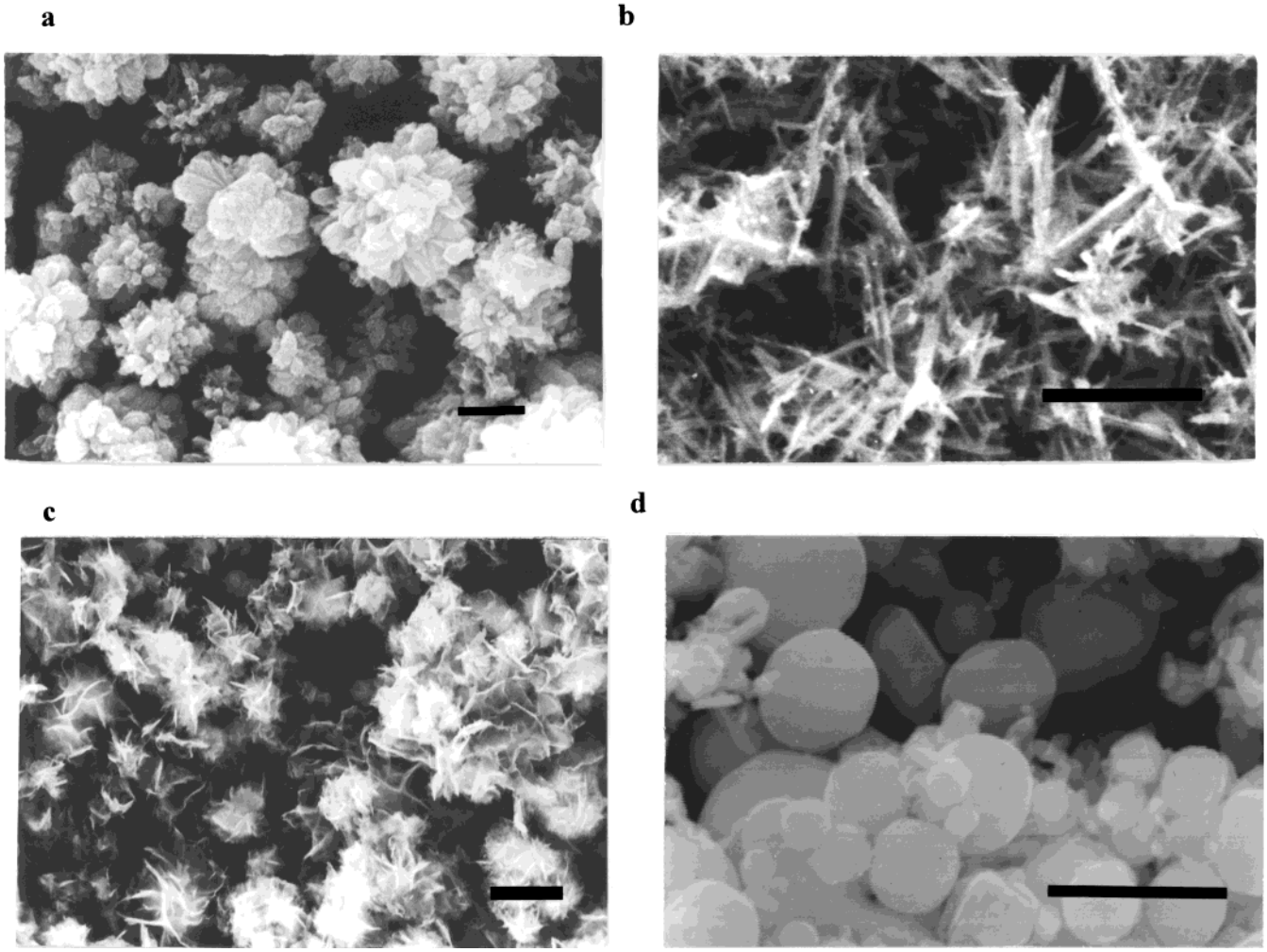

Figure 6. SEM images of submicrometric Bi_2S_3 particles prepared in (a) *p*-xylene (bar = 0.5 μm), (b) 2-ethoxyethanol (bar = 1 μm), (c) 4-ethylpyridine (bar = 0.5 μm), and (d) TOPO/TOP (bar = 0.5 μm).

To establish the morphological properties of the Bi_2S_3 nanoparticulates, TEM was performed on samples collected from a CH_2Cl_2 solution containing Bi_2S_3, which were deposited on carbon-coated copper grids. Figure 4 shows that the Bi_2S_3 powders prepared in 2-ethoxyethanol are composed of nanoparticles with a fiberlike morphology and with an average linear cross-section dimension of ca. 6 nm. The low contrast of the TEM images also suggests that the sample consists of very thin particles of Bi_2S_3. As reported by others for several colloidal layered semiconductors,[17,18,40,41] it is reasonable to suggest that because of the lamellar-like structure of Bi_2S_3, such particles are in fact layers of the semiconductor. In this case, and as suggested in Figure 4, the TEM images agree with the presence of Bi_2S_3 nanocrystals with a linear dimension for which quantum size effects are expected to be observed. It also seems that such quantum size effects are observed, even though the length of the particles, the largest linear dimension, surpasses the nanosize regime. In this context it is noteworthy that quantum size effects have also been reported by Variano et al. for Bi_2S_3 disklike-shaped particles prepared in microemulsions, for which the anisotropic particle-in-a-box model has been applied.[12] Compared to nanocrystals of other semiconductors (e.g., II/VI materials) in which quantum confinement occurs in a three-dimension box,[42] the charge carriers in anisotropic lamellar nanostructures are confined in a quantum structure defined by two (disk-type) or one (fiber-type) linear dimensions.[12,18]

Although the fiber-type morphology predominates for Bi_2S_3 particles prepared using the method reported here, it was observed that the particle dimensions were strongly dependent on the synthetic parameters used in their preparation, in particular, the type of solvent used and the growth temperature. Typically, larger fibers were obtained in ethyleneglycol and the dimensions of the fibers increased as the temperature was raised. For example, the TEM image in Figure 5 shows Bi_2S_3 nanoparticles (ca. 24-nm linear cross section) prepared in ethyleneglycol (197 °C) using the single-molecule precursor $[Bi(S_2CNMe^nHex)_3(C_{12}H_8N_2)]$ (**2**). Longer fibers were obtained using this precursor, when compared to the use of precursor **1**, although a similar morphology was observed, providing the solvent and the temperature were maintained. The thermal analysis of the molecular precursors **1** and **2** showed that both compounds thermally decompose in one step. The lower temperature of decomposition of **2** (280 °C), when

(40) Peterson, M. W.; Micic, O. I.; Nozik, A. J. *J. Phys. Chem*. **1988**, *92*, 4160.
(41) Wilcoxon J. P.; Samara, G. A. *Phys. Rev. B* **1995**, *51*, 7299.
(42) Brus, L. E. *J. Chem Phys*. **1984**, *80*, 4403.

compared to **1** (300 °C), may account for such slight differences in the particles size, although the precursors' thermal stabilities are not so pronounced as to lead to a strong influence on the final morphology of the Bi_2S_3 nanocrystals. On the other hand, the influence of the solvent and temperature on the morphology of the powders was also clearly evident by SEM performed on the nondispersible solid phases collected from the thermalysis of the molecular precursors. Figure 6 shows the SEM images of such powders, which have been prepared in *p*-xylene (a), 2-ethoxyethanol (b), 4-ethylpyridine (c), and TOPO (d). The predominance of fiber-type particles is again observed in all the samples with the exception of the one prepared in TOPO in which elemental bismuth was also present. For this sample, the elemental bismuth particles were also analyzed by TEM and transmission electron diffraction, performed on the dispersible powders (nanophase material), showing either a hexagonal or spherical shape. When *p*-xylene is used, which is a noncoordinating solvent, steric hindrance of the particles is less effective and hence agglomerates of smaller particles have been formed, as discussed above (Figure 6a).

Bismuth(III) sulfide crystallizes in a layer structure formed from threadlike molecules. The crystallization occurs in a two-dimensional array forming infinite bands, which are connected via weaker van der Waals interactions. The Bi_2S_3 fiber-type morphology observed for the powders may result from the cleavage of larger particles from the van der Waals planes of the crystalline structure or/and from preferential directional growth of the particles. In fact, both processes have been reported to occur for Bi_2S_3 particles grown using distinct synthetic methods.[43,44] Temperature exerts a strong influence on the morphology of particles in which preferential growth is a relevant process and this experimental parameter was investigated for the solvent ethyleneglycol. As shown in Figure 7, distinct morphologies for micrometric Bi_2S_3 particles were obtained depending on the temperature used, 132 and 197 °C. Such SEM images suggest that the morphological evolution of the particles is to obtain longer fibers as the temperature increases, which may result from a higher growth rate along the *c* axis. Solvent thermalysis of commercial Bi_2S_3 over 2 h, using similar conditions to those used in the synthesis of the nanocrystalline counterpart, did not lead to fiber-type particles. It has been reported that treatment of macrocrystalline lamellar semiconductors (e.g., MoS_2, WS_2, Bi_2Se_3) in acetonitrile results in stable nanodispersed systems.[45] The breakup of crystallites due to interpenetration of acetonitrile molecules within the van der Waals planes has been suggested as the underlying mechanism. The Bi−S interatomic distance at the van der Waals planes is ca. 300 pm; hence, an exfoliation process by intercalation of larger molecules, such as those of the solvents used in this work, seems unlikely. Moreover, the fiber-type morphology has been observed by us for Bi_2S_3 particles prepared using several chemical strategies, including a chemical vapor deposition method in which the molecular precursors used were similar to those employed in this work.[22] Therefore, it is suggested that the Bi_2S_3 fiber-type morphology for particles prepared from the decomposition of bismuth(III) dithiocarbamato complexes is mainly a result of preferential directional growth along the *c* axis, the shortest distance of the unit cell of bismuthinite.

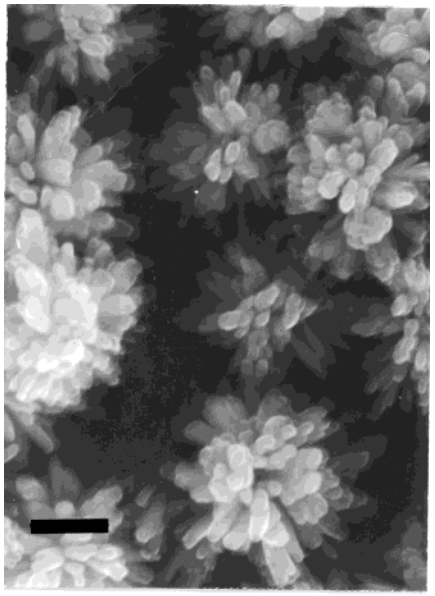

a

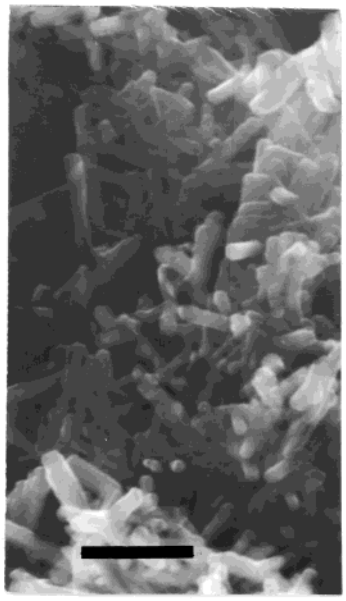

b

Figure 7. SEM images of submicrometric Bi_2S_3 particles prepared in ethyleneglycol at (a) 132 and (b) 197 °C (bar = 0.3 μm).

4. Conclusions

It was shown that crystalline Bi_2S_3 nano- and microparticles showing well-defined morphologies can be prepared using the solution-phase thermalysis of bismuth(III) alkyldithiocarbamato complexes. The tem-

(43) Mizoguchi, H.; Hosono, H.; Ueda, N.; Kawazoe, H. *J. Appl. Phys*. **1995**, *78*, 1376.
(44) Yu, S.; Shu, L.; Yang, J.; Han, Z.; Qian, Y.; Zhang, Y. *J. Mater. Res*. **1999**, *14*, 4157.
(45) Comor, M. I.; Dramicanin, M. D.; Rakocevic, Z.; Zec, S.; Nedeljkovic, J. M. *J. Mater. Sci. Lett.* **1998**, *17*, 1401.

perature and chemical nature of the solvent used have a strong influence on the final properties of the powders. Particle growth along the *c* axis appears to be a preferential process leading to Bi_2S_3 particulates in which the fiber-type morphology is predominant.

Acknowledgment. We thank Fundação para a Ciência e a Tecnologia (FCT) (Project POCTI/1999/CTM/35458). O.C.M. thanks FCT for a Ph.D. grant. We thank Mr. A. Lopes for his expertise on the TEM analysis and Professor Paul O'Brien (University of Manchester) for helpful discussions.

Supporting Information Available: Crystal data and structure refinement, atomic coordinates and equivalent isotropic displacement parameters, bond lengths and angles, anisotropic displacement parameters, hydrogen coordinates and isotropic displacement parameters, and structures of compounds **1** and **2** (PDF). This material is available free of charge via the Internet at http://pubs.acs.org.

CM000973Y